This document is a preprint of: P. Neuhaus, M. Schlüter, C. Jans, *et al.*, "Enabling energy-efficient Tbit/s communications by 1-bit quantization and oversampling," in *Proc. Joint European Conf. on Networks and Commun. & 6G Summit (EuCNC/6G Summit)*, Virtual Conference (Porto, Portugal), Jun. 2021, pp. 84–89. DOI: 10.1109/EuCNC/6GSummit51104.2021.9482427.

Enabling Energy-Efficient Tbit/s Communications by 1-Bit Quantization and Oversampling

Peter Neuhaus, Martin Schlüter, Christoph Jans, Meik Dörpinghaus, and Gerhard Fettweis
Vodafone Chair Mobile Communications Systems, Technische Universität Dresden, 01062 Dresden, Germany
{peter_friedrich.neuhaus, martin.schlueter, christoph.jans, meik.doerpinghaus, gerhard.fettweis}@tu-dresden.de

***Abstract*—In this work, we investigate the energy efficiency (EE) of future wireless communications systems. We argue that operating at high bandwidth and a comparatively low signal-to-noise ratio (SNR) is beneficial in terms of EE. Furthermore, we discuss how employing single-carrier modulations combined with 1-bit quantization and temporal oversampling at the receiver enables energy-efficient wideband wireless communications systems. Our main contribution is to compare the EE of such a system to an idealized conventional system under various assumptions on the ADC power consumption. Our numerical results suggest that the EE can be improved significantly by employing 1-bit quantization and oversampling at the receiver at the cost of increased bandwidth.**

***Index Terms*—energy efficiency, wideband systems, 1-bit, quantization, oversampling**

I. Introduction

With the ever-increasing demand for faster communications systems, data rates in the order of terabits per second will be required soon. Leveraging modern silicon technologies' performance, recently demonstrated front-end hardware for millimeter-wave (mmWave) wireless communications systems have peak data rates that exceed $100\,\mathrm{Gbit/s}$ [1]. In general, enabling terabit wireless communications systems with data rates beyond $100\,\mathrm{Gbit/s}$ implies using huge channel bandwidths, which are available in the sub-terahertz (THz) frequency bands above $100\,\mathrm{GHz}$. Especially the frequency range outside of 170-210 GHz is promising since the average atmospheric attenuation is, e.g., approx. $0.002\,\mathrm{dB/m}$ at $300\,\mathrm{GHz}$, which is sufficiently small considering short-range communications [2, Fig. 3].

Designing receivers for data rates in the order of $100\,\mathrm{Gbit/s}$ poses new challenges since high bandwidths imply high sampling rates and, thus, analog-to-digital converters (ADCs) become a major energy consumption bottleneck. For sampling frequencies above $300\,\mathrm{MHz}$, the energy per conversion step increases linearly with the frequency, while for lower sampling rates, the energy per conversion step is independent of the sampling rate [3], [4]. To circumvent this problem, we consider 1-bit quantization enabling power savings due to, e.g., reduced linearity requirements on the receiver and possibly allowing to omit the automatic gain control. A further advantage is that the supply voltage of the ADC circuits can be decreased below $1\,\mathrm{V}$ as much less voltage headroom for amplitude processing is required [5]. In order to recover some of the information that is lost due to 1-bit quantization, we consider oversampling at the receiver, i.e., we trade amplitude resolution for time resolution. This combination of 1-bit quantization and oversampling is a perfect match for nm-scale semiconductor processes that have a decreased voltage range but allow for a high temporal resolution (e.g., GlobalFoundries FDX22 operates at 0.4-$0.8\,\mathrm{V}$ with $f_{\max} \approx 370\,\mathrm{GHz}$ [6]). In fact, it is argued in [3] that technology scaling has greatly benefited low-to-moderate resolution ADCs, but brings no direct benefit for high-resolution ADCs.

An example for the application of 1-bit ADCs for communications systems with very high bandwidths is the design of energy-efficient high performance compute nodes with wireless board-to-board communication [7]. Another possible example are future wireless local area networks (LANs), where the coverage would be limited to a single room, e.g., in a factory hall or at home. Due to the high carrier frequencies, the signal cannot pass through walls [8] and thus no interference is caused to or by other communication systems.

An energy-efficient ADC parametrization for wideband communications systems has been investigated in [9], where it was found that a high sampling rate and a very low amplitude resolution usually results in the highest energy efficiency (EE) for a fixed throughput. Enablers for energy-efficient communications systems for frequencies above $90\,\mathrm{GHz}$ have been studied in [10], where the authors proposed to revisit single-carrier modulations to increase spectral efficiency (SE) and EE.

The remainder of this work is organized as follows: First, in Sec. II, we argue on theoretical grounds that in terms of EE it is beneficial to operate at large bandwidths and at comparatively low signal-to-noise ratios (SNRs), which implies operating with a low SE. Then, in Sec. III, we discuss practical advantages of single-carrier over multi-carrier modulations for wideband systems. In Sec. IV, we briefly review the practical wideband single-carrier zero-crossing modulation (ZXM) communications system from [11], which employs 1-bit quantization and oversampling at the receiver. Afterwards, in Sec. V and Sec. VI, we discuss the ADC power consumption and show that the considered wideband ZXM system can achieve a significantly higher EE as compared to a conventional system, at the cost of an increased bandwidth. Finally, conclusions are drawn in Sec. VII.

This work has been supported in part by the German Research Foundation (DFG) in the Collaborative Research Center "Highly Adaptive Energy-Efficient Computing", SFB 912, HAEC, Project-ID 164481002 and in part by the German Federal Ministry of Education and Research (BMBF) (project E4C, contract number 16ME0189). Computations were performed at the Center for Information Services and High Performance Computing (ZIH) at TU Dresden.

This document is a preprint of: P. Neuhaus, M. Schlüter, C. Jans, *et al.*, "Enabling energy-efficient Tbit/s communications by 1-bit quantization and oversampling," in *Proc. Joint European Conf. on Networks and Commun. & 6G Summit (EuCNC/6G Summit)*, Virtual Conference (Porto, Portugal), Jun. 2021, pp. 84–89. DOI: 10.1109/EuCNC/6GSummit51104.2021.9482427.

II. Bandwidth vs. SNR

In the preceding section, we have argued that to achieve very high data rates, possible larger than $100\,\mathrm{Gbit/s}$, it is more reasonable to choose a higher bandwidth than a high ADC resolution. Putting the technological advantages aside, choosing a high bandwidth can also be justified on purely theoretical grounds. Let us start with the bandlimited complex-valued additive white Gaussian noise (AWGN) channel

$$\mathsf{y}(t) = (\mathsf{x}(t) + \mathsf{n}(t)) * g_{\mathrm{ideal}}(t), \tag{1}$$

where $\mathsf{x}(t)$ denotes the signal waveform, $\mathsf{n}(t)$ denotes white Gaussian noise and $g_{\mathrm{ideal}}(t)$ is an ideal rectangular low pass filter with one-sided bandwidth W. The capacity of this channel is given by [12, Sec. 3.3]

$$C_{\mathrm{AWGN}} = 2W\log_2\left(1 + \frac{P}{2WN_0}\right)\,[\mathrm{bit/s}], \tag{2}$$

where P and N_0 denote the transmit power and noise spectral density, respectively, such that the SNR is defined as $\mathrm{SNR} \triangleq \frac{P}{2WN_0}$. It is a well-known fact that the rate by which the capacity increases at large values of P is logarithmic. If W and P are increased such that the ratio $\frac{P}{W}$ remains constant, then the capacity increases linearly. Thus, putting more power in the same amount of bandwidth and thereby increasing the SE, given by $\frac{C_{\mathrm{AWGN}}}{2W}$, is less effective than spreading additional power over more bandwidth and keeping the SE constant. The higher the SNR, the more pronounced is the loss in capacity compared to a system with lower SNR but equal transmit power and higher bandwidth.

To quantify this, let us consider two systems. The first system has bandwidth W such that its capacity is given by

$$C_1 = 2W\log_2\left(1 + \mathrm{SNR}_1\right)\,[\mathrm{bit/s}], \tag{3}$$

where $\mathrm{SNR}_1 = \frac{P}{2WN_0}$. The second system uses the same transmit power P and operates on the same noise spectral density N_0, but utilizes a bandwidth αW whereby its capacity is

$$C_2 = 2\alpha W\log_2\left(1 + \frac{\mathrm{SNR}_1}{\alpha}\right)\,[\mathrm{bit/s}]. \tag{4}$$

Let us now assume, without loss of generality, that the second system scales its bandwidth with $\alpha = \mathrm{SNR}_1$. In this case, the ratio of the two capacities is given by

$$\frac{C_1}{C_2} = \frac{2W\log_2\left(1 + \mathrm{SNR}_1\right)}{2\mathrm{SNR}_1 W\log_2\left(1 + \frac{\mathrm{SNR}_1}{\mathrm{SNR}_1}\right)} = \frac{\log_2\left(1 + \mathrm{SNR}_1\right)}{\mathrm{SNR}_1}. \tag{5}$$

From (5) we observe that for $\mathrm{SNR}_1 > 0\,\mathrm{dB}$, the second system always achieves a higher capacity than the first system, and the gap widens with increasing transmit power.

As discussed in the preceding section, our goal is to design communications receivers based on ADCs with 1-bit quantization to enable very high bandwidths. For the communications system design, it is thus essential to know the capacity in case 1-bit quantization is applied at the receiver, i.e., we want to know the capacity of the channel with input $\mathsf{x}(t)$ and output $\mathsf{r}(t)$, given by

$$\mathsf{r}(t) = \mathrm{sign}\left(\mathrm{Re}\left\{\mathsf{y}(t)\right\}\right) + j\,\mathrm{sign}\left(\mathrm{Im}\left\{\mathsf{y}(t)\right\}\right), \tag{6}$$

where $\mathrm{sign}\,(x) = 1$ if $x > 0$ and $\mathrm{sign}\,(x) = -1$ if $x \leq 0$. Assuming Nyquist rate sampling with period $T_{\mathrm{N}} \triangleq \frac{1}{2W}$, we can apply the discussion of [13, Sec. 9.3] to [14, Lemma 1] such that

$$C_{1-\mathrm{bit,Nyq.}} = 4W\left(1 - H_b\left(Q\left(\sqrt{\frac{P}{N_0 W}}\right)\right)\right)\,[\mathrm{bit/s}], \tag{7}$$

where $H_b(\cdot)$ denotes the binary entropy function and $Q(\cdot)$ is the Gaussian Q-function. As intuitively expected, the capacity is achieved by quadrature phase-shift keying (QPSK) signaling and for $\mathrm{SNR} \to \infty$ the SE is $2\,\mathrm{bit/s/Hz}$.

Even in situations where the bandwidth can be made very large, the maximum available bandwidth is always limited, either by the regulator or simply by technological limits. In case the SE of $2\,\mathrm{bit/s/Hz}$ achievable by QPSK modulation is not sufficient to achieve the target data rate and additional transmit power is available, the question arises if the SE can be increased while using 1-bit quantization at the receiver. It is essential to understand that with only 1-bit of amplitude resolution, the information must be conveyed in the time domain, i.e., in the temporal distances between zero-crossings (ZXs) of the transmit signal. The higher the time resolution of the 1-bit ADC the more information can be transmitted within the ZX time differences of the transmit signal. We thus effectively trade amplitude resolution for time resolution, which is much easier to achieve in nm-scale semiconductor processes. This concept was termed ZXM in [15].

Computing the capacity of the 1-bit quantized channel (6) with arbitrary sampling rate is rather complicated and still an open problem. For the noiseless case, lower bounds on the achievable rate when oversampling a real-valued bandlimited process with a specific construction are given in [16]. One of the bounds is

$$I_{\mathrm{LB}} = \log_2\left(1 + \frac{f_{\mathrm{s}}}{2W}\right)\,[\mathrm{bit/T_N}], \tag{8}$$

where f_{s} denotes the sampling rate. This suggests that oversampling enables SEs above $2\,\mathrm{bit/s/Hz}$, achievable with QPSK and Nyquist sampling. This fact motivated the work in [17] where practical modulation schemes in combination with 1-bit quantization and oversampling at the receiver were shown to achieve the bound (8) for high SNR. A promising approach is linear modulation with QPSK symbols in combination with sequence design and faster-than-Nyquist (FTN) signaling [18]. A system based on run-length limited (RLL) sequences, which are a natural choice if information must be conveyed in the time domain, is described in Sec. IV.

III. Single-Carrier vs. Multi-Carrier

In our work, we favor a single-carrier over a multi-carrier system because we typically operate in a sparse scattering geometrical environment at such high frequencies. The sparse channel results from the large attenuation for frequencies above $100\,\mathrm{GHz}$, following from Friis' law, and the usage of highly directive antennas at both, the transmitter and the receiver, to compensate for it [8].

Therefore, an arriving electromagnetic wave interacts only with few scatterers, resulting in a small set of multi-path components [19]. After spatial filtering and beam alignment on

This document is a preprint of: P. Neuhaus, M. Schlüter, C. Jans, *et al.*, "Enabling energy-efficient Tbit/s communications by 1-bit quantization and oversampling," in *Proc. Joint European Conf. on Networks and Commun. & 6G Summit (EuCNC/6G Summit)*, Virtual Conference (Porto, Portugal), Jun. 2021, pp. 84–89. DOI: 10.1109/EuCNC/6GSummit51104.2021.9482427.

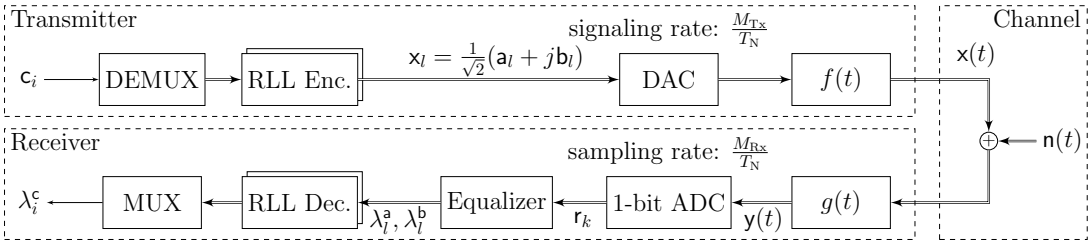

Fig. 1. Overview of the system model, where c_i corresponds to input bits to be transmitted and λ_i^{c} to the corresponding log-likelihood ratios at the receiver.

both sides, we obtain a single-tap, i.e., frequency flat, single-input single-output effective channel [19, Sec. II.C]. In accordance with this and supported by measurement campaigns [20], we can claim that the effective channel response remains approx. constant over the duration of many symbols and can, hence, be described by a *time-invariant* single-tap channel due to low mobility in the considered scenarios.

Under such conditions, multi-carrier systems, with their sensitivity towards hardware impairments (power amplifier non-linearities, carrier frequency offsets, phase noise, etc.), are not recommendable [21], [22]. Furthermore, the generally lower peak-to-average power ratio (PAPR) of single-carrier modulations compared to multi-carrier waveforms enables an improved PA efficiency. It is also known that in a channel with only a few or even a single tap, the distortion caused by 1-bit quantization degrades the performance of multi-carrier systems much more than that of single carrier systems [23]. Therefore, it is reasonable to assume that a low-cost, energy-efficient system is based on a single-carrier modulation scheme employing spatial filtering on both sides to concentrate its signal power and concurrently mitigates intersymbol interference (ISI).

IV. 1-bit Communications System

Following the arguments from Sec. II and Sec. III, we briefly describe a practical implementation of a single-carrier ZXM system in the remainder of this section. To this aim, we consider the system proposed in [11], which employs 1-bit quantization and temporal oversampling at the receiver. However, for simplicity, we assume an AWGN channel. The system model is illustrated in Fig. 1.

A. Transmit Signal

As mentioned above, the considered system employs ZXM [15], which is implemented based on the combination of FTN signaling with RLL transmit sequences [17]. FTN signaling can be understood as increasing the symbol rate at the transmitter, i.e., employing a symbol spacing of $\frac{T_{\mathrm{N}}}{M_{\mathrm{Tx}}}$, where $M_{\mathrm{Tx}} \in [1, \infty)$ denotes the FTN signaling factor [18]. Intuitively, employing FTN signaling allows creating ZXs on a finer grid, thus, increasing the transmission data rate. However, FTN signaling, i.e., choosing $M_{\mathrm{Tx}} > 1$, comes at the cost of self-introduced ISI.

To combat the ISI due to FTN signaling, we combine it with RLL transmit sequences, which are known from magnetic and optical storage systems [24]. RLL sequences are binary bipolar sequences with a positive and a negative amplitude, typically ± 1, which are constraint, such that the same polarization has to be kept for at least $d+1$ and at most $k+1$ consecutive symbols. The k constraint is omitted in this work, i.e., we set $k \triangleq \infty$, which maximizes the rate.

Hence, the continuous-time transmit signal is given by

$$\mathsf{x}(t) = \sum_{l=1}^{m} \mathsf{x}_l \, f\left(t - \frac{lT_{\mathrm{N}}}{M_{\mathrm{Tx}}}\right), \tag{9}$$

where the Nyquist interval T_{N} is defined by the root-raised-cosine (RRC) transmit filter $f(t)$, and x_l denotes the lth element of $\mathbf{x}^m$, which is given by $\mathbf{x}^m \triangleq \frac{1}{\sqrt{2}}(\mathbf{a}^m + j\mathbf{b}^m)$, where $\mathbf{a}^m, \mathbf{b}^m \in \{+1, -1\}^m$ denote two independently modulated RLL sequences. Note that encoding and decoding of bits onto RLL sequences is performed using the finite-state machine (FSM) RLL codes which where derived in [11]. Following the configuration proposed in [11], we choose integer FTN signaling factors, i.e., $M_{\mathrm{Tx}} \in \mathbb{N}$, and choose the RLL d constraint as $d = M_{\mathrm{Tx}} - 1$. Note that in this case $M_{\mathrm{Tx}} = 1$ corresponds to standard QPSK signalling, because the RLL constraint is effectively omitted, i.e., $d = 0$.

B. Received Signal

The received signal is given by

$$\mathsf{y}(t) = (\mathsf{x}(t) + \mathsf{n}(t)) * g(t), \tag{10}$$

where $g(t)$ denotes a RRC receive filter, matched to the transmit filter $f(t)$. Sampling $\mathsf{y}(t)$ with rate $\frac{M_{\mathrm{Rx}}}{T_{\mathrm{N}}}$, where M_{Rx} denotes the temporal oversampling factor w.r.t. the Nyquist rate, yields

$$\mathsf{y}_k = \sum_{l=1}^{m} \mathsf{x}_l \, v\left(\frac{kT_{\mathrm{N}}}{M_{\mathrm{Rx}}} - \frac{lT_{\mathrm{N}}}{M_{\mathrm{Tx}}}\right) + (\mathsf{n} * g)\left(\frac{kT_{\mathrm{N}}}{M_{\mathrm{Rx}}}\right), \tag{11}$$

where $\mathsf{n}(t)$ denotes a circularly-symmetric complex AWGN process and $v(t) \triangleq (f * g)(t)$ denotes the combined transmit and receive filter. Afterwards, 1-bit quantization is applied independently to the real and imaginary part of the received signal, which yields $\mathsf{r}_k = \mathrm{sign}\left(\mathrm{Re}\left\{\mathsf{y}_k\right\}\right) + j\mathrm{sign}\left(\mathrm{Im}\left\{\mathsf{y}_k\right\}\right)$. Combining all 1-bit quantized samples into a single vector yields $\mathbf{r}^{\bar{m}} = [\mathsf{r}_1, \ldots, \mathsf{r}_{\bar{m}}]^T$ with $\bar{m} = m \cdot M$, where $M = \frac{M_{\mathrm{Rx}}}{M_{\mathrm{Tx}}}$ denotes the effective oversampling factor w.r.t. the signaling rate, which is assumed to be integer, i.e., $M \in \mathbb{N}$.

C. Receiver

At the receiver, the equalizer first performs approximate maximum a posteriori (MAP) symbol detection of the RLL symbols a_l and b_l. This can be implemented efficiently using the Bahl-Cocke-Jelinek-Raviv (BCJR) algorithm [25]. Details

This document is a preprint of: P. Neuhaus, M. Schlüter, C. Jans, *et al.*, "Enabling energy-efficient Tbit/s communications by 1-bit quantization and oversampling," in *Proc. Joint European Conf. on Networks and Commun. & 6G Summit (EuCNC/6G Summit)*, Virtual Conference (Porto, Portugal), Jun. 2021, pp. 84–89. DOI: 10.1109/EuCNC/6GSummit51104.2021.9482427.

on the implementation can be found in [11]. Then, the equalizer provides soft-information for each real-valued RLL symbol, in the form of log-likelihood ratios (LLRs), where λ_l^{a} and λ_l^{b} denote the LLRs w.r.t. a_l and b_l, respectively.

Afterwards, again using the BCJR algorithm, the RLL decoder implements soft-input soft-output decoding of the considered FSM RLL codes. The decoder provides soft-information in the form of LLRs, denoted as λ_i^{c}, per information bit c_i at the RLL encoder input. The SE of this system has been investigated in [26] by numerically approximating the mutual information $I(\mathsf{c}_i;\lambda_i^{\mathsf{c}})$ under the assumption of i.i.d. input bits c_i.

V. ADC Power Dissipation

In this section, we review ADC power dissipation. We are particularly interested in the scaling behaviour of the ADC power consumption P_{ADC} with the input bandwidth $2W$, with the amplitude resolution b, and with oversampling $M_{\mathrm{Rx}} \triangleq \frac{f_{\mathrm{s}}}{2W}$.

An analytical lower bound on the ADC power consumption for a single Nyquist rate ADC is obtained in [27, eq. (5)]

$$P_{\mathrm{ADC,LB}} = 48 \cdot k_{\mathrm{B}} T \cdot 2W \cdot 2^{2\mathrm{ENOB}}\,[\mathrm{W}], \qquad (12)$$

where k_{B} denotes the Boltzmann constant, T the absolute temperature and ENOB denotes the effective number of bits. The bound in (12) is derived under the assumption that the sampling noise power equals the quantization noise power. Under this assumption, the effective resolution can be obtained as $\mathrm{ENOB} = b - 0.5$, where b denotes the ADC amplitude resolution in bits. From (12), it follows that the power consumption grows linearly in the input bandwidth and exponentially in the effective resolution, i.e., $P_{\mathrm{ADC,LB}} \propto 2W$ and $P_{\mathrm{ADC,LB}} \propto 2^{2\mathrm{ENOB}}$. However, in practice, the lower bound in (12) is rather loose [27].

An extensive ADC performance survey is provided in [4]. This survey reveals the following scaling behaviour of practical ADC implementations: *i)* The power consumption scales linearly with the input bandwidth for $2W \leq 336\,\mathrm{MHz}$ and quadratically for $2W > 336\,\mathrm{MHz}$. The reason for this is given in [3]: "[T]he transistors have to be driven *harder* to push against transit frequency limitations of the process." *ii)* For low amplitude resolutions b, the power consumption P_{ADC} scales with $P_{\mathrm{ADC}} \propto 2^{\mathrm{ENOB}}$, whereas for moderate and high resolutions, it scales with $P_{\mathrm{ADC}} \propto 2^{2\mathrm{ENOB}}$, which is consistent with the behaviour of noise-limited analog circuits [28].

In *time-interleaved* ADC architectures, which are popular for high-speed converters, a set of identical parallel ADCs is fed by time-delayed inputs, such that the individual sub-ADCs can operate at a lower rate [29]. In line with this architecture, we assume that the power consumption is proportional to the oversampling factor M_{Rx}, i.e., $P_{\mathrm{ADC}} \propto M_{\mathrm{Rx}}$.

Combining the findings above yields the following model for the overall scaling behaviour of the ADC power consumption:

$$P_{\mathrm{ADC}} \propto M_{\mathrm{Rx}} \cdot (2W)^{\nu} \cdot 2^{\zeta \mathrm{ENOB}}, \quad \nu, \zeta \in \{1, 2\}, \qquad (13)$$

where ν takes into account the different scaling for frequencies below and above 336 MHz and ζ takes into account the different scaling for low and high amplitude resolutions. Note that a quadratic scaling in $2W$ and a linear scaling in M_{Rx} is not necessarily a contradiction because the quadratic scaling with $2W$ is caused by the increased input bandwidth, whereas the linear increase in M_{Rx} is motivated by a time-interleaved architecture.

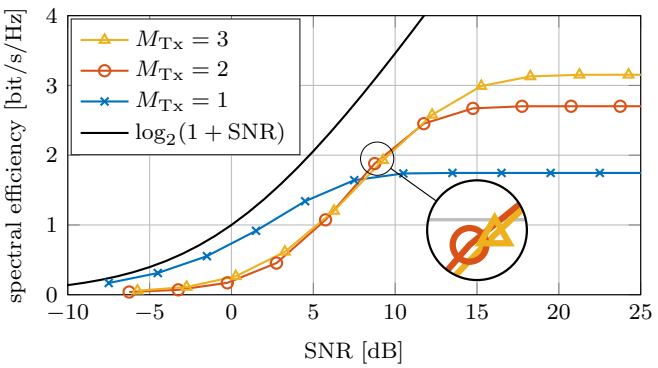

Fig. 2. SE evaluation of the considered ZXM system w.r.t. the 95 % power containment bandwidth for $M = 3$ and $d = M_{\mathrm{Tx}} - 1$. Results from [26].

VI. Numerical Results

In this section, we compare the EE of the considered ZXM system employing 1-bit quantization and temporal oversampling (cf. Sec. IV) to an idealized conventional system, operating with a low bandwidth and a high SE, hence, requiring a high ADC amplitude resolution. To this end, we utilize the SE results obtained in [26] w.r.t. the 95 % power containment bandwidth, i.e., the results allow for 5 % out-of-band emissions of the ZXM system[1]. The system's SE is depicted in Fig. 2. Note that employing FTN signaling, i.e., choosing $M_{\mathrm{Tx}} > 1$, is only beneficial for SNRs above approx. 7.5 dB. Based on these results, the data rate of a ZXM system can be obtained by

$$R_{\mathrm{ZXM}}(\mathrm{SNR}_{\mathrm{ZXM}}) = 2W_{\mathrm{ZXM}}\,\mathrm{SE}(\mathrm{SNR}_{\mathrm{ZXM}})\,[\mathrm{bit/s}], \qquad (14)$$

where $\mathrm{SNR}_{\mathrm{ZXM}}$, W_{ZXM} and $\mathrm{SE}(\mathrm{SNR}_{\mathrm{ZXM}})$ denote the SNR, the one-sided bandwidth and the SE of the ZXM system, respectively. Note that $\mathrm{SE}(\mathrm{SNR}_{\mathrm{ZXM}})$ is given in Fig. 2.

Then, we compare the performance of the ZXM system to an *idealized* conventional system: Similar to Sec. II, we approximate the performance of the idealized conventional system by the AWGN capacity and scale the bandwidth of the conventional system, such that both systems achieve equal data rates and utilize equal transmit powers, i.e.,

$$\begin{aligned} R_{\mathrm{ZXM}}(\mathrm{SNR}_{\mathrm{ZXM}}) &= 2\alpha W_{\mathrm{ZXM}} \log_2\left(1 + \frac{\mathrm{SNR}_{\mathrm{ZXM}}}{\alpha}\right) \\ &\triangleq R_{\mathrm{conv}}(\mathrm{SNR}_{\mathrm{conv}})\,[\mathrm{bit/s}], \end{aligned} \qquad (15)$$

where the one-sided bandwidth and the SNR of the conventional system are given by $W_{\mathrm{conv}} \triangleq \alpha W_{\mathrm{ZXM}}$ and $\mathrm{SNR}_{\mathrm{conv}} \triangleq \frac{\mathrm{SNR}_{\mathrm{ZXM}}}{\alpha}$, respectively. The bandwidth scaling factor $\alpha > 0$ in (15) is obtained numerically using the bisection method [30, Sec. 2.1]. In Fig. 3, we compare the required bandwidth of the two systems. It can be seen that for $\mathrm{SNR}_{\mathrm{ZXM}} \geq 0\,\mathrm{dB}$, there exists a ZXM system configuration which requires only approx. $2-3$ times more bandwidth than the conventional system to achieve the same data rate.

[1]Note that even though the work [26] considers a wideband line-of-sight channel, the SE results are effectively obtained for an AWGN channel.

This document is a preprint of: P. Neuhaus, M. Schlüter, C. Jans, *et al.*, "Enabling energy-efficient Tbit/s communications by 1-bit quantization and oversampling," in *Proc. Joint European Conf. on Networks and Commun. & 6G Summit (EuCNC/6G Summit)*, Virtual Conference (Porto, Portugal), Jun. 2021, pp. 84–89. DOI: 10.1109/EuCNC/6GSummit51104.2021.9482427.

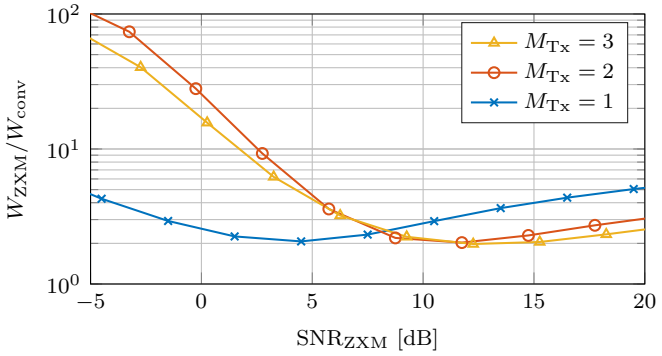

Fig. 3. Comparison of the required bandwidth of the considered ZXM system to an idealized conventional system, where both systems achieve equal data rates and utilize equal transmit powers.

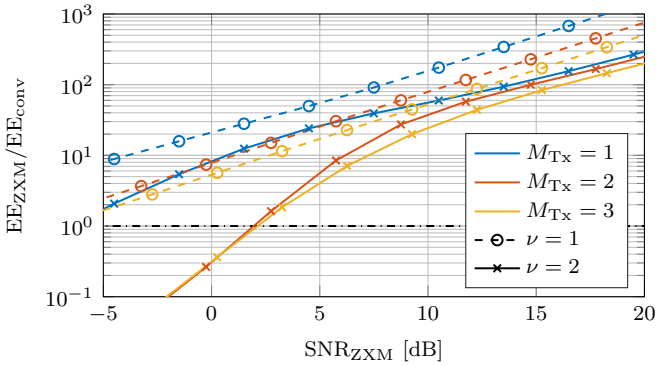

Fig. 4. EE comparison for $\zeta = 2$ and $\Xi = 3$ under the assumption of a linear and quadratic scaling of the ADC power consumption with the input bandwidth $2W$, i.e., for $\nu = 1$ and $\nu = 2$, respectively.

Next, we compare the EE of the two systems, where we only take into account the ADC power consumption, which is assumed to dominate the overall power consumption. Note that the power dissipation of the remaining components can be assumed identical for both systems due to equal transmit powers and data rates. Hence, we define the EE as

$$\mathrm{EE}_{\mathcal{X}} \triangleq \frac{R_{\mathcal{X}}}{2\,P_{\mathrm{ADC},\mathcal{X}}}\ [\mathrm{bit/J}], \quad \mathcal{X} \in \{\mathrm{ZXM}, \mathrm{conv}\}, \tag{16}$$

where the factor 2 in the denominator is due to one ADC per real signaling dimension. Utilizing (15) and (16), we obtain

$$\frac{\mathrm{EE}_{\mathrm{ZXM}}}{\mathrm{EE}_{\mathrm{conv}}} = \frac{P_{\mathrm{ADC,conv}}}{P_{\mathrm{ADC,ZXM}}} \overset{\text{(a)}}{=} \frac{M_{\mathrm{Rx,conv}} \cdot \alpha^{\nu} \cdot 2^{\zeta(b_{\mathrm{conv}}-0.5)}}{M_{\mathrm{Rx,ZXM}} \cdot 2^{(b_{\mathrm{ZXM}}-0.5)}}, \tag{17}$$

where (a) is due to (13) and due to $\zeta = 1$ for the ZXM system because of a low ADC resolution. Furthermore, b_{conv} and $b_{\mathrm{ZXM}} \triangleq 1$ denote the ADC resolution of the conventional and the ZXM system, respectively. Moreover, we assume that the conventional system requires an amplitude resolution of

$$b_{\mathrm{conv}} \triangleq \frac{\mathrm{SE}_{\mathrm{conv}}(\mathrm{SNR}_{\mathrm{conv}})}{2} + \Xi, \tag{18}$$

which is sufficient to approximate the performance of an unquantized system. For example, for a trellis-coded 8-PSK system with rate $2/3$, an amplitude resolution of $b_{\mathrm{conv}} = 4$ is sufficient [31], i.e., this suggests $\Xi = 3$. Furthermore, we assume $M_{\mathrm{Rx,conv}} = 2$ in the following, which is required for fully digital timing synchronization based on samples from a free running clock [12, Secs. 4.2.4., 5.4, and 5.5]. For the ZXM system we assume $M_{\mathrm{Rx,ZXM}} = 3M_{\mathrm{Tx}}$, which is expected to be sufficient for timing synchronization [32].

In Fig. 4 we evaluate the EE ratio, given in (17), for $\zeta = 2$ and $\Xi = 3$ under the assumption of a linear and quadratic scaling of the ADC power consumption with the input bandwidth $2W$, i.e., for $\nu = 1$ and $\nu = 2$, respectively (cf. Sec. V). The ZXM system is much more energy-efficient over a wide range of SNRs, e.g., at $\mathrm{SNR}_{\mathrm{ZXM}} = 5\,\mathrm{dB}$ and $\mathrm{SNR}_{\mathrm{ZXM}} = 10\,\mathrm{dB}$, the ZXM system is at least approx. 4 and approx. 20 times more energy-efficient. The gain of the ZXM system is even larger for $\nu = 1$, because the additionally utilized bandwidth is less expensive in terms of ADC power consumption, as compared

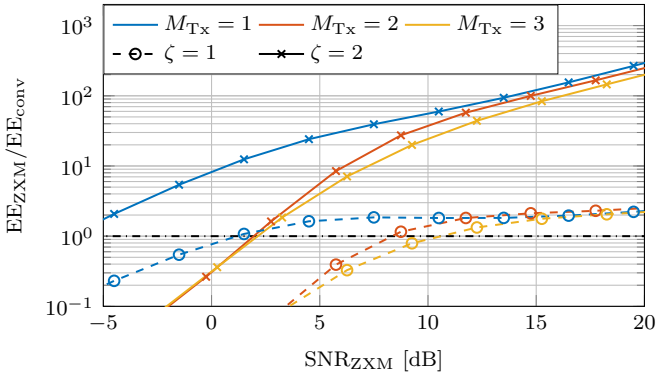

Fig. 5. EE comparison for $\nu = 2$ and $\Xi = 3$ under the assumption that the power consumption doubles or quadruples for each integer increase in EBNO, i.e., for $\zeta = 1$ and $\zeta = 2$, respectively.

to the case $\nu = 2$. In general, the ZXM system is expected to utilize a large bandwidth, hence, the assumption $\nu = 2$ is expected to resemble practical systems more closely.

Then, in Fig. 5 we evaluate the EE ratio for $\nu = 2$ and $\Xi = 3$ under the assumption that the power consumption doubles or quadruples for each integer increase in EBNO in the conventional system, i.e., for $\zeta = 1$ and $\zeta = 2$, respectively (cf. Sec. V). Compared to $\zeta = 2$, the gain in energy efficiency is significantly reduced for $\zeta = 1$. However, for $\mathrm{SNR}_{\mathrm{ZXM}}$ above approx. $10\,\mathrm{dB}$ the ZXM system is still more energy-efficient. As discussed in Sec. V, the assumption $\zeta = 1$ is valid for low amplitude resolutions, hence it is expected that $\zeta = 2$ resembles the behaviour of conventional systems more closely, as they typically operate with high resolutions.

Finally, we evaluate the EE ratio for $\nu = 2$ and $\zeta = 2$ when reducing Ξ in Fig. 6. Even for $\Xi = 1$, i.e., under the assumption that the conventional system requires only a single additional bit over the SE for implementation, the ZXM system is more energy-efficient for $\mathrm{SNR}_{\mathrm{ZXM}} > 10\,\mathrm{dB}$.

In summary, when comparing the conventional and ZXM systems, we show the potential for significant EE gains due to employing 1-bit quantization and temporal oversampling. Furthermore, evaluating the specific ZXM implementation from [11], the 1-bit quantized QPSK system, i.e., employing $M_{\mathrm{Tx}} = 1$,

This document is a preprint of: P. Neuhaus, M. Schlüter, C. Jans, *et al.*, "Enabling energy-efficient Tbit/s communications by 1-bit quantization and oversampling," in *Proc. Joint European Conf. on Networks and Commun. & 6G Summit (EuCNC/6G Summit)*, Virtual Conference (Porto, Portugal), Jun. 2021, pp. 84–89. DOI: 10.1109/EuCNC/6GSummit51104.2021.9482427.

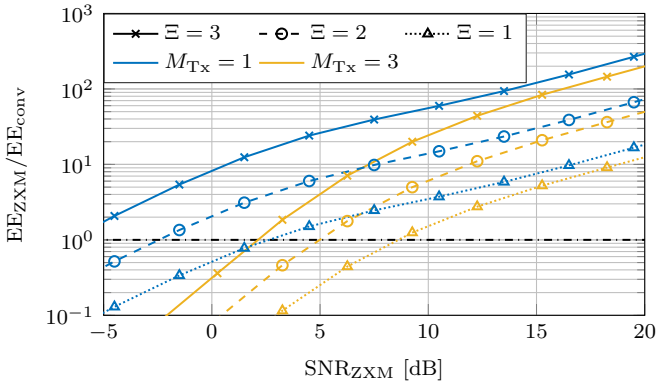

Fig. 6. Evaluating different assumptions on Ξ in (18) for $\nu = 2$ and $\zeta = 2$.

is nearly always the most energy-efficient. However, for SNRs above approx. 7.5 dB, it can be beneficial to employ FTN signaling because this achieves a higher SE (cf. Fig. 2) and, thus, requires less bandwidth (cf. Fig. 3) while still providing significant EE gains. Enhanced ZXM implementations could achieve even higher gains at possibly lower SNRs (cf. [17]). Note that the shown gains in EE are obtained only taking into account the ADC power consumption (cf. (16)). Consequently, the presented results do not necessarily imply that we can increase the systems' overall EE by orders of magnitude. However, they indicate that the ADC power consumption can be reduced significantly.

VII. Conclusions

In this work, we discussed how to enable energy-efficient future wireless communications systems by utilizing a large bandwidth, operating at low SNR, using single-carrier modulation, and employing 1-bit quantization and temporal oversampling at the receiver. We compared the EE of the ZXM system from [11] to an idealized conventional system. Our numerical results showed that the 1-bit temporal oversampling system can significantly outperform a conventional system in terms of EE under a wide range of assumptions on the ADC power consumption. Extending the work by taking into account interference, e.g., due to multiple users, is left for future work.

References

[1] K. K. Tokgoz, S. Maki, J. Pang, N. Nagashima, I. Abdo *et al.*, "A 120Gb/s 16QAM CMOS millimeter-wave wireless transceiver," in *Proc. IEEE Int. Solid-State Circuits Conf.*, vol. 61, San Francisco, CA, USA, Mar. 2018, pp. 168–170.

[2] J. Wells, "Faster than fiber: The future of multi-Gb/s wireless," *IEEE Microw. Mag.*, vol. 10, no. 3, pp. 104–112, May 2009.

[3] B. Murmann, "Energy limits in A/D converters," in *Proc. 2013 IEEE Faible Tension Faible Consommation*, Paris, France, Jun. 2013, pp. 1–4.

[4] ——, "ADC performance survey 1997-2020," http://web.stanford.edu/ murmann/adcsurvey.html, Aug. 2020.

[5] R. B. Staszewski, "Digitally intensive wireless transceivers," *IEEE Des. Test Comput.*, vol. 29, no. 6, pp. 7–18, Dec. 2012.

[6] S. N. Ong, S. Lehmann, W. H. Chow, C. Zhang, C. Schippel *et al.*, "A 22nm FDSOI technology optimized for RF/mmWave applications," in *Proc. IEEE Radio Freq. Integr. Circuits Symp.*, Philadelphia, PA, USA, Jun. 2018, pp. 72–75.

[7] G. P. Fettweis, M. Dörpinghaus, J. Castrillon, A. Kumar, C. Baier *et al.*, "Architecture and advanced electronics pathways toward highly adaptive energy-efficient computing," *Proc. IEEE*, vol. 107, no. 1, pp. 204–231, Jan. 2019.

[8] R. W. Heath, N. González-Prelcic, S. Rangan, W. Roh, and A. M. Sayeed, "An overview of signal processing techniques for millimeter wave MIMO systems," *IEEE J. Sel. Areas Commun.*, vol. 10, no. 3, pp. 436–453, Apr. 2016.

[9] S. Krone and G. Fettweis, "Energy-efficient A/D conversion in wideband communications receivers," in *Proc. IEEE Veh. Technol. Conf. (VTC Fall)*, San Francisco, CA, USA, Sep. 2011, pp. 1–5.

[10] J. Doré, Y. Corre, S. Bicais, J. Palicot, E. Faussurier *et al.*, "Above-90GHz spectrum and single-carrier waveform as enablers for efficient Tbit/s wireless communications," in *Proc. Int. Conf. on Telecommun. (ICT)*, St. Malo, France, June 2018, pp. 274–278.

[11] P. Neuhaus, M. Dörpinghaus, H. Halbauer, S. Wesemann, M. Schlüter *et al.*, "Sub-THz wideband system employing 1-bit quantization and temporal oversampling," in *Proc. IEEE Int. Conf. Commun. (ICC)*, Dublin, Ireland, Jun. 2020, pp. 1–7.

[12] H. Meyr, M. Moeneclaey, and S. Fechtel, *Digital Communication Receivers: Synchronization, Channel Estimation, and Signal Processing*. New York, NY, USA: John Wiley & Sons, Inc., 1997.

[13] T. M. Cover and J. A. Thomas, *Elements of Information Theory*. New York, NY, USA: John Wiley & Sons, 2006.

[14] J. Mo and R. W. Heath, "Capacity analysis of one-bit quantized MIMO systems with transmitter channel state information," *IEEE Trans. Signal Process.*, vol. 63, no. 20, pp. 5498–5512, Oct. 2015.

[15] G. Fettweis, M. Dörpinghaus, S. Bender, L. Landau, P. Neuhaus, and M. Schlüter, "Zero crossing modulation for communication with temporally oversampled 1-bit quantization," in *Proc. Asilomar Conf. Signals, Systems, and Computers*, Pacific Grove, CA, USA, Nov. 2019, pp. 207–214.

[16] S. Shamai, "Information rates by oversampling the sign of a bandlimited process," *IEEE Trans. Inf. Theory*, vol. 40, no. 4, pp. 1230–1236, Jul. 1994.

[17] L. T. N. Landau, M. Dörpinghaus, and G. P. Fettweis, "1-bit quantization and oversampling at the receiver: Sequence-based communication," *EURASIP J. Wireless Commun. Netw.*, vol. 2018, no. 1, p. 83, 2018.

[18] J. E. Mazo, "Faster-than-Nyquist signaling," *Bell Syst. Tech. J.*, vol. 54, no. 8, pp. 1451–1462, Oct. 1975.

[19] X. Song, S. Haghighatshoar, and G. Caire, "Efficient beam alignment for millimeter wave single-carrier systems with hybrid MIMO transceivers," *IEEE Trans. Wireless Commun.*, vol. 18, no. 3, pp. 1518–1533, Mar. 2019.

[20] M. R. Akdeniz, Y. Liu, M. K. Samimi, S. Sun, S. Rangan *et al.*, "Millimeter wave channel modeling and cellular capacity evaluation," *IEEE J. Sel. Areas Commun.*, vol. 32, no. 6, pp. 1164–1179, June 2014.

[21] S. Buzzi, C. D'Andrea, T. Foggi, A. Ugolini, and G. Colavolpe, "Single-carrier modulation versus OFDM for millimeter-wave wireless MIMO," *IEEE Trans. Commun.*, vol. 66, no. 3, pp. 1335–1348, Mar. 2018.

[22] B. Akgun, M. Krunz, and D. Manzi, "Impact of beamforming on delay spread in wideband millimeter-wave systems," in *Proc. Int. Conf. Comput. Netw. Commun. (ICNC)*, Big Island, HI, USA, Feb. 2020, pp. 890–896.

[23] C. Mollen, J. Choi, E. G. Larsson, and R. W. Heath, "Uplink performance of wideband massive MIMO with one-bit ADCs," *IEEE Trans. Wirel. Commun.*, vol. 16, no. 1, pp. 87–100, Jan. 2017.

[24] K. A. S. Immink, "Runlength-limited sequences," *Proc. IEEE*, vol. 78, no. 11, pp. 1745–1759, Nov. 1990.

[25] L. Bahl, J. Cocke, F. Jelinek, and J. Raviv, "Optimal decoding of linear codes for minimizing symbol error rate (corresp.)," *IEEE Trans. Inf. Theory*, vol. 20, no. 2, pp. 284–287, Mar. 1974.

[26] P. Neuhaus, M. Dörpinghaus, H. Halbauer, V. Braun, and G. Fettweis, "On the spectral efficiency of oversampled 1-bit quantized systems for wideband LOS channels," in *Proc. IEEE Int. Symp. on Personal, Indoor and Mobile Radio Commun. (PIMRC)*, London, U.K., Aug. 2020, pp. 1–6.

[27] T. Sundstrom, B. Murmann, and C. Svensson, "Power dissipation bounds for high-speed Nyquist analog-to-digital converters," *IEEE Trans. Circuits Syst. I, Reg. Papers*, vol. 56, no. 3, pp. 509–518, Mar. 2009.

[28] B. Murmann, "The race for the extra decibel: A brief review of current ADC performance trajectories," *IEEE Solid State Circuits Mag.*, vol. 7, no. 3, pp. 58–66, Sep. 2015.

[29] W. C. Black and D. A. Hodges, "Time interleaved converter arrays," *IEEE J. Solid-State Circuits*, vol. 15, no. 6, pp. 1022–1029, Dec. 1980.

[30] R. L. Burden and D. J. Faires, *Numerical Analysis*. Boston, MA, USA: Brooks/Cole, 2011.

[31] O. Joeressen, M. Oerder, R. Serra, and H. Meyr, "DIRECS: system design of a 100 Mbit/s digital receiver," *IEE Proc. G Circuits, Devices Syst.*, vol. 139, no. 2, p. 222, Apr. 1992.

[32] M. Schlüter, M. Dörpinghaus, and G. P. Fettweis, "NDA timing estimation with 1-bit quantization and oversampling at the receiver," in *Proc. IEEE Glob. Commun. Conf.*, Taipei, Taiwan, Dec. 2020, pp. 1–6.